Computational Biology and Bioinformatics
2020; 8(2): 77-89
http://www.sciencepublishinggroup.com/j/cbb
doi: 10.11648/j.cbb.20200802.17
ISSN: 2330-8265 (Print); ISSN: 2330-8281 (Online)

Bioinformatics Analysis Identifies Potential Key Genes of Peripheral Blood Mononuclear Cell in Idiopathic Pulmonary Fibrosis

Lijun Liu[1], Daxia Cai[2], Yi Wu[1, *]

[1]Department of Respiratory Medicine, The First Affiliated Hospital of Jinan University, Guangzhou, China

[2]Institute of Hematology, Jinan University, Guangzhou, China

Email address:
twuyi@jnu.edu.cn (Yi Wu)

[*]Corresponding author

To cite this article:
Lijun Liu, Daxia Cai, Yi Wu. Bioinformatics Analysis Identifies Potential Key Genes of Peripheral Blood Mononuclear Cell in Idiopathic Pulmonary Fibrosis. *Computational Biology and Bioinformatics.* Vol. 8, No. 2, 2020, pp. 77-89. doi: 10.11648/j.cbb.20200802.17

Received: November 4, 2020; **Accepted**: November 17, 2020; **Published**: November 27, 2020

Abstract: Idiopathic pulmonary fibrosis (IPF) is a chronic progressive fibrotic interstitial pneumonia with progressive worsening of dyspnea and lung function. The etiology of IPF is unknown, and the pathogenesis remains unclear. Our study aimed to investigate the key genes of the peripheral blood mononuclear cell in IPF by bioinformatics analysis. Our study used the online Gene Expression Omnibus (GEO) microarray expression profiling dataset GSE28042 to identify differentially expressed genes (DEGs) between IPF patients and healthy controls. We performed the Gene Ontology (GO) and pathway enrichment analyses of genes for annotation, visualization, and integrated discovery. The STRING database constructed Protein-protein interaction (PPI) network analysis, and hub genes were identified by the CytoHubba plugin. Moreover, we used the receiver operating characteristic (ROC) curve to assess the diagnostic value of the hub genes. In total, 28 upregulated and 44 downregulated genes were identified in the differential expression analysis. The protein-protein interaction network (PPI) was established with 69 nodes and 68 edges. The top 10 hub genes were JUN, FOS, STAT3, SOCS3, JUNB, DUSP1, IL4, FCER1A, MS4A2, and CPA3. Kyoto Encyclopedia of Genes and Genomes (KEGG) pathways enriched for the important module containing hub genes contained Fc epsilon RI signaling pathway, TNF signaling pathway, Jak-STAT signaling pathway, and MAPK signaling pathway. Additionally, the identified hub genes show high functional similarity and diagnostic value in IPF. Our study used bioinformatics analysis to provide new insight into the mechanisms underlying IPF. However, more experiments are needed to explore the relationships between the top 10 hub genes and IPF in the future.

Keywords: Bioinformatic Analysis, Genes, Peripheral Blood Mononuclear Cell, Idiopathic Pulmonary Fibrosis

1. Introduction

Idiopathic pulmonary fibrosis (IPF) is defined as a specific form of chronic, progressive fibrosing interstitial pneumonia and its cause is unknown [1]. Its clinical features are unexplained exertional dyspnea, chronic dry cough, or Velcro rale on examination [2]. The histopathology of this disease is interstitial fibrosis with spatial heterogeneity and patchy involvement of lung parenchyma, and microscopic honeycombing [3]. The incidence of IPF is high and its incidence rates increased over time in most countries. Its incidence ranges from 0.2 per 100000 per year to 93.7 per 100000 per year based on estimates from Europe and North America [4]. Besides, median survival from the time of diagnosis is only 2.5 to 3.5 years [5]. Currently, the risk factors of IPF are environmental, genetic, epigenetic alterations, and aging [6]. However, the pathogenesis is still not exact.

So far, understanding of the pathogenesis of IPF includes epithelial cell dysfunction caused by genetic susceptibility, defined profibrotic processes caused by TGF-beta activation, and progressive pulmonary fibrosis [7, 8]. However, recent studies have shown that epithelial cell dysfunction is still a central cause of IPF [7]. Currently, the diagnosis of IPF requires exclusion of other known causes of interstitial disease (ILD), high-resolution, and surgical lung biopsy [1]. However, the accuracy of the diagnosis of IPF requires experienced

physicians, which has certain limitations. IPF patients are usually in the terminal stages of the disease when diagnosed and there is no particularly effective treatment at this point. Therefore, early diagnosis and early treatment were most important.

Bioinformatics analyses can enable researchers to search online biological databases to explore the pathogenesis and molecular diagnosis, such as juvenile dermatomyositis [9], major depressive disorder [10], Tuberculosis [11]. Here, we use the peripheral blood mononuclear cell (PBMC) microarray dataset GSE28042 created by Herazo-Maya et al. to investigated the differentially expressed genes (DEGs) between IPF patients and healthy controls to explore the key genes. Our findings will provide new insights into the clinical diagnosis and treatment of IPF.

2. Materials and Methods

2.1. Microarray Data

The microarray data of GSE28042 was downloaded from the Gene Expression Omnibus (GEO, http://www.ncbi.nlm.nih,gov/geo/) database. The dataset was based on the GPL6480 Agilent-014850 Whole Human Genome Microarray 4x44K G4112F (Probe Name Version). The data type was expression profiling by the array and the species selected was *Homo sapiens*. The peripheral blood mononuclear cell samples (PBMC) included 75 patients with the diagnosis of IPF (IPF group) and 19 healthy controls (control group). The clinical details of GSE28042 were listed (Table 1). The annotation file for GPL6480 was also downloaded from the GEO.

Table 1. *Clinical information of GSE28042 included cases.*

	All subjects	IPF group	Control group
Patients	94	75	19
Gender			
Male	64	52	12
Female	30	23	7
Age (years)	65.84±10.63	69.00±8.16	53.37±10.23

2.2. Analysis of Differentially Expressed Genes (DEGs)

We used the online analysis tool GEO2R (http://www.ncbi.nlm.nih.gov/geo/geo2r/) to screen the DEGs between the IPF group and the control group. The GEO2R can allow us to compare two or more groups of samples to identify genes that are differentially expressed across experimental conditions. The results are presented as a table of genes ordered by significance. To exclude gender differences, we divided the IPF group and the control group into two groups (Male IPF group, Female IPF group, Male control group, Female control group), respectively, depending on the gender. *P*-values and adjusted *P*-values (adj. *p*) were calculated using *t*-tests. Genes with log2 fold change (FC) >1 and adj. p <0.05 were identified as DEGs. A Venn diagram of DEGs was drawn using the online tool Venny 2.1 (http://bioinfogp.cnb.csic.es/tools/venny/). The heatmap for the DEGs was created using R software (version 4.0.2).

2.3. Gene Ontology (GO) and Pathway Enrichment Analysis of DEGs

GO, a bioinformatics tool aims to establish a vocabulary that defines and describes the functions of genes and proteins for a variety of species. GO is divided into three parts: Molecular Function (MF), Biological Process (BP), and Cellular Component (CC) [12]. KEGG (Kyoto Encyclopedia of Genes and Genomes) is a database that systematically analyzes the metabolic pathways of gene products in cells and their functions [13]. KEGG integrates data on genomes, chemical molecules, and biochemical systems, including metabolic pathways, drugs, diseases, genes, and genomes [13]. The Database for Annotation, Visualization, and Integrated Discovery (DAVID; http://david.ncifcrf.gov; version 6.8) is a free online biological information database and it provides a comprehensive set of functional annotation tools for researchers to understand biological meaning behind a large list of genes. We performed GO and KEGG pathway enrichment analyses using the DAVID online database to analyze the function of DEGs. *P*-value <0.05 was set as the cut-off criteria.

2.4. Protein-protein Interaction (PPI) Network Analysis and Module Analysis

A significant number of proteins do not function alone. Proteins interact with each other to form complexes that then do their work. We used the Search Tool for the Retrieval of Interacting Genes (STRING; https://string-db.org/; version 11.0) online database to systematically predict and construct a PPI network of all DEGs. A combined score >0.4 of PPI pairs was regarded as a significant interaction. Cytoscape (version 3.8.0), a bioinformatic software available online, can be used to construct and visualize the network of PPI. MCODE (version 1.5.1), a plugin of Cytoscape software, can construct functional modules by clustering in a large network of PPI. CytoHubba, mainly used for exploring PPI network hub genes, is a Cytoscape plugin. We selected the genes with the highest ranking by the maximum correlation criterion (MCC). The selected genes are represented by redder color.

2.5. Go and Pathway Enrichment Analysis of Hub Genes

To analyze the function of hub genes, biological analyses were performed using the DAVID online database. *P*-value <0.05 was set as the cut-off criteria.

2.6. Hub Genes Diagnostic Efficacy Evaluation

The receiver operating characteristic (ROC) curve can be used to assess the diagnostic accuracy. We use the "pROC" package of the R software to plot the ROC curve, calculate the area under the curve (AUC) and evaluate the diagnostic capability of hub genes to distinguish IPF patients and healthy controls.

2.7. Statistical Analysis

All statistical analyses were performed as the

means±standard deviation. The R software (version 4.0.2) was used to analyze the data. A *P*-value <0.05 was considered statistically significant.

3. Results

3.1. Differentially Expressed Genes

We downloaded the microarray expression dataset GSE28042 from the GEO database and analyzed the DEGs between IPF patients and healthy controls using the GEO2R tool. In total, 107 upregulated and 244 downregulated genes were identified between male IPF patients and male healthy controls. Besides, 54 upregulated and 212 downregulated genes were identified between female IPF patients and female healthy controls. The intersection of these two datasets identified 28 upregulated and 44 downregulated genes (Table 2). The Venn diagram and heatmap for the DEGs are presented in Figure 1.

Table 2. *Differentially expressed genes of IPF.*

Gene Symbol	ID	adj. P. Val		P. Value	
		male	female	male	female
Upregulated genes					
AP1S1	A_23_P157404	0.000121	0.0297	0.000001	0.000515
AP1S1	A_24_P63950	0.000674	0.0262	0.0000156	0.000391
AP5B1	A_24_P9883	0.000151	0.0037	0.00000139	0.00000307
APOL6	A_24_P941167	0.00146	0.0367	0.0000538	0.000798
COQ10B	A_32_P1192	0.00116	0.0299	0.0000369	0.00052
DUSP1	A_23_P110712	0.0000000888	0.0179	0.0000000000329	0.000163
EMP1	A_24_P921446	0.0000652	0.0225	0.000000357	0.000262
FAM20A	A_32_P108254	0.00000741	0.0244	0.0000000132	0.000314
FAM20A	A_24_P352952	0.0000433	0.023	0.00000019	0.000278
FCAR	A_24_P348265	0.0000142	0.0132	0.0000000356	0.0000787
FOS	A_23_P106194	0.00000000612	0.000409	0.000000000001	0.0000000824
GSTT2	A_23_P109427	0.00684	0.0173	0.000523	0.000151
JUN	A_23_P201538	0.00000000514	0.00507	0.00000000000069	0.0000074
JUNB	A_24_P241815	0.0000117	0.0139	0.0000000255	0.000091
LMNB1	A_23_P258493	0.00227	0.0305	0.000103	0.000545
MBD2	A_24_P119201	0.000408	0.0471	0.00000652	0.00148
PDAP1	A_23_P151198	0.00216	0.0382	0.0000948	0.000884
PDK4	A_23_P257087	0.00119	0.0128	0.0000386	0.0000717
PDK4	A_24_P243749	0.00132	0.00476	0.0000465	0.00000655
PEAK1	A_24_P933801	0.000244	0.0081	0.00000299	0.0000188
PER1	A_24_P93916	0.00000534	0.0126	0.00000000824	0.0000641
RHOB	A_23_P51136	0.00000000749	0.00363	0.00000000000176	0.00000268
SERPINB2	A_23_P153185	0.000491	0.0159	0.00000886	0.000127
SLED1	A_24_P927716	0.0001	0.0346	0.000000721	0.000711
SOCS3	A_23_P207058	0.000000918	0.0111	0.000000000694	0.0000478
SOCS3	A_23_P351069	0.0000018	0.00738	0.0000000017	0.0000129
SOD2	A_24_P935819	0.0000179	0.0226	0.000000051	0.000265
SRGN	A_24_P915269	0.0000000042	0.00287	0.000000000000259	0.00000154
STAC3	A_23_P10947	0.00000318	0.0081	0.00000000384	0.0000186
STAT3	A_24_P923962	0.0001	0.0108	0.000000715	0.0000403
TEX14	A_32_P126079	0.00395	0.0181	0.000235	0.000175
TMEM107	A_23_P118791	0.0000914	0.0225	0.000000631	0.000262
Downregulated genes					
ABCC13	A_23_P397480	0.0366	0.0257	0.00593	0.000371
C10orf82	A_23_P1286	0.000338	0.0291	0.00000487	0.000497
C1orf186	A_23_P95640	0.00000435	0.0294	0.00000000584	0.000505
CACNG6	A_23_P501933	0.000000956	0.045	0.000000000802	0.00131
CCDC85A	A_23_P349566	0.0115	0.0111	0.00113	0.0000453
CCR3	A_23_P250302	0.000000207	0.0108	0.000000000111	0.000041
CCR3	A_24_P367473	0.0000879	0.0465	0.000000575	0.00142
CD24	A_23_P85250	0.0102	0.0244	0.000929	0.000312
CLC	A_23_P101683	0.0000306	0.0376	0.000000119	0.00085
CPA3	A_23_P18017	0.0000000888	0.0195	0.0000000000387	0.000197
ENPP3	A_23_P404536	0.00000018	0.0181	0.0000000000906	0.000179
EPB42	A_23_P140675	0.0319	0.0195	0.00483	0.000196
FCER1A	A_23_P103765	0.000395	0.0382	0.0000062	0.000883
FCRLA	A_24_P276576	0.00319	0.0402	0.00017	0.00102
GPR37	A_23_P145995	0.0336	0.0167	0.00522	0.000142

Gene Symbol	ID	adj. P. Val		P. Value	
		male	female	male	female
HBA1	A_23_P37856	0.000805	0.00511	0.0000208	0.00000772
HBA2	A_24_P142305	0.000431	0.0037	0.00000734	0.00000348
HBA2	A_23_P26457	0.000599	0.0039	0.0000127	0.00000458
HBD	A_24_P75190	0.000588	0.00976	0.0000123	0.0000265
HBQ1	A_23_P49254	0.00166	0.000147	0.0000637	0.0000000197
HDC	A_23_P117662	0.0000212	0.0173	0.0000000718	0.000154
HRH4	A_23_P386310	0.000244	0.0122	0.00000301	0.0000592
IL4	A_23_P213706	0.000000062	0.014	0.0000000000208	0.0000965
ITGB8	A_24_P759477	0.00000686	0.00752	0.000000012	0.0000146
LTK	A_23_P14853	0.000151	0.0249	0.00000138	0.000334
MME	A_24_P260101	0.00147	0.0122	0.000054	0.0000581
MME	A_23_P212061	0.00345	0.00622	0.000191	0.0000102
MPPED2	A_23_P52888	0.000459	0.0252	0.00000803	0.000342
MS4A2	A_23_P1904	0.00000277	0.0143	0.00000000316	0.000106
PAGE2	A_32_P70927	0.0227	0.0151	0.00299	0.000118
PAGE2B	A_32_P109683	0.0301	0.0211	0.00445	0.000226
PAGE5	A_23_P22744	0.0288	0.0139	0.00419	0.0000912
RAB3IP	A_32_P180920	0.0000206	0.0254	0.0000000656	0.00035
RBM20	A_24_P453497	0.00119	0.0453	0.0000387	0.00134
RNF182	A_23_P399255	0.00802	0.0433	0.000659	0.00119
SLC45A3	A_24_P208345	0.0000106	0.0247	0.0000000227	0.000321
SLC4A10	A_24_P930111	0.0000133	0.0373	0.0000000311	0.000822
SLC4A10	A_24_P314786	0.0000429	0.0481	0.000000186	0.00158
THSD7A	A_24_P400324	0.0000000888	0.0037	0.0000000000381	0.00000347
TRIM49	A_23_P1575	0.000000918	0.0184	0.000000000719	0.000182
TRIM51	A_23_P150483	0.0000000042	0.00984	0.000000000000282	0.0000282
TRIM53AP	A_24_P16353	0.00000825	0.00131	0.000000015	0.000000396
TRIM64	A_23_P12972	0.000508	0.0271	0.00000939	0.000425
TRPM6	A_23_P216712	0.00000528	0.0138	0.00000000779	0.0000885
UGT2B11	A_23_P212968	0.00777	0.0367	0.000628	0.000802
UGT2B7	A_23_P136671	0.000353	0.000000111	0.00000525	0.00000000000373
VWCE	A_23_P52986	0.0252	0.00742	0.00346	0.0000142
ZNF91	A_23_P209146	0.0000181	0.0108	0.0000000522	0.000042

Table 2. *Continued.*

Gene Symbol	ID	log FC		Gene. title
		male	female	
Upregulated genes				
AP1S1	A_23_P157404	1.1140727	1.2453211	adaptor related protein complex 1 sigma 1 subunit
AP1S1	A_24_P63950	1.0989288	1.2347777	adaptor related protein complex 1 sigma 1 subunit
AP5B1	A_24_P9883	1.6985578	1.5936472	adaptor related protein complex 5 beta 1 subunit
APOL6	A_24_P941167	1.5528797	1.6845138	apolipoprotein L6
COQ10B	A_32_P1192	1.1098125	1.4745875	coenzyme Q10B
DUSP1	A_23_P110712	2.2050261	1.7767065	dual specificity phosphatase 1
EMP1	A_24_P921446	1.293242	1.2217363	epithelial membrane protein 1
FAM20A	A_32_P108254	1.9548785	1.5243216	family with sequence similarity 20 member A
FAM20A	A_24_P352952	2.0801823	1.6580721	family with sequence similarity 20 member A
FCAR	A_24_P348265	1.5712738	1.1219079	Fc fragment of IgA receptor
FOS	A_23_P106194	2.8185477	2.8510469	Fos proto-oncogene, AP-1 transcription factor subunit
GSTT2	A_23_P109427	1.076046	1.2621832	glutathione S-transferase theta 2 (gene/pseudogene)
JUN	A_23_P201538	2.3210056	2.2608329	Jun proto-oncogene, AP-1 transcription factor subunit
JUNB	A_24_P241815	1.4505145	1.4068335	JunB proto-oncogene, AP-1 transcription factor subunit
LMNB1	A_23_P258493	1.2516538	1.6254543	lamin B1
MBD2	A_24_P119201	1.6597378	1.6667309	methyl-CpG binding domain protein 2
PDAP1	A_23_P151198	1.1131674	1.3884275	PDGFA associated protein 1
PDK4	A_23_P257087	1.0898457	1.6686671	pyruvate dehydrogenase kinase 4
PDK4	A_24_P243749	1.0776004	1.6681819	pyruvate dehydrogenase kinase 4
PEAK1	A_24_P933801	1.1617162	1.2234933	pseudopodium enriched atypical kinase 1
PER1	A_24_P93916	2.5128018	1.6856721	period circadian clock 1
RHOB	A_23_P51136	1.8707196	1.4680517	ras homolog family member B
SERPINB2	A_23_P153185	1.075777	1.0828608	serpin family B member 2

Gene Symbol	ID	log FC		Gene. title
		male	female	
SLED1	A_24_P927716	2.2508577	2.0327458	proteoglycan 3 pseudogene
SOCS3	A_23_P207058	2.1650652	1.7844297	suppressor of cytokine signaling 3
SOCS3	A_23_P351069	1.9930166	1.7282561	suppressor of cytokine signaling 3
SOD2	A_24_P935819	2.1525682	2.2469801	superoxide dismutase 2, mitochondrial
SRGN	A_24_P915269	2.1742154	2.6417286	serglycin
STAC3	A_23_P10947	1.1117068	1.0203305	SH3 and cysteine rich domain 3
STAT3	A_24_P923962	1.0796424	1.2121782	signal transducer and activator of transcription 3
TEX14	A_32_P126079	1.2880819	1.7212135	testis expressed 14, intercellular bridge forming factor
TMEM107	A_23_P118791	1.4412015	1.4721218	transmembrane protein 107
Downregulated genes				
ABCC13	A_23_P397480	-1.951228	-2.946519	ATP binding cassette subfamily C member 13 (pseudogene)
C10orf82	A_23_P1286	-1.867092	-1.680199	chromosome 10 open reading frame 82
C1orf186	A_23_P95640	-1.620385	-1.214304	chromosome 1 open reading frame 186
CACNG6	A_23_P501933	-2.489393	-2.006053	calcium voltage-gated channel auxiliary subunit gamma 6
CCDC85A	A_23_P349566	-1.066576	-1.840001	coiled-coil domain containing 85A
CCR3	A_23_P250302	-2.382942	-2.10451	C-C motif chemokine receptor 3
CCR3	A_24_P367473	-1.410334	-1.052858	C-C motif chemokine receptor 3
CD24	A_23_P85250	-1.011483	-1.195061	CD24 molecule
CLC	A_23_P101683	-2.57649	-2.635986	Charcot-Leyden crystal galectin
CPA3	A_23_P18017	-2.455389	-1.959501	carboxypeptidase A3
ENPP3	A_23_P404536	-1.88905	-1.296145	ectonucleotide pyrophosphatase/phosphodiesterase 3
EPB42	A_23_P140675	-1.985546	-3.31249	erythrocyte membrane protein band 4.2
FCER1A	A_23_P103765	-1.316214	-1.139695	Fc fragment of IgE receptor Ia
FCRLA	A_24_P276576	-1.056556	-1.299941	Fc receptor like A
GPR37	A_23_P145995	-1.190649	-1.960249	G protein-coupled receptor 37
HBA1	A_23_P37856	-2.165281	-2.768918	hemoglobin subunit alpha 1
HBA2	A_24_P142305	-2.755512	-3.783318	hemoglobin subunit alpha 2
HBA2	A_23_P26457	-2.317402	-2.940702	hemoglobin subunit alpha 2
HBD	A_24_P75190	-2.138927	-2.707546	hemoglobin subunit delta
HBQ1	A_23_P49254	-2.358415	-3.671391	hemoglobin subunit theta 1
HDC	A_23_P117662	-2.252604	-2.297751	histidine decarboxylase
HRH4	A_23_P386310	-1.84512	-2.35102	histamine receptor H4
IL4	A_23_P213706	-2.436502	-2.315922	interleukin 4
ITGB8	A_24_P759477	-2.315214	-1.795095	integrin subunit beta 8
LTK	A_23_P14853	-1.084265	-1.088327	leukocyte receptor tyrosine kinase
MME	A_24_P260101	-1.706598	-2.295779	membrane metallo-endopeptidase
MME	A_23_P212061	-1.405164	-2.026871	membrane metallo-endopeptidase
MPPED2	A_23_P52888	-1.656583	-1.338681	metallophosphoesterase domain containing 2
MS4A2	A_23_P1904	-2.626586	-2.433001	membrane spanning 4-domains A2
PAGE2	A_32_P70927	-1.139398	-1.566661	PAGE family member 2
PAGE2B	A_32_P109683	-1.185484	-1.926982	PAGE family member 2B
PAGE5	A_23_P22744	-1.058192	-1.493009	PAGE family member 5
RAB3IP	A_32_P180920	-1.021236	-1.452316	RAB3A interacting protein
RBM20	A_24_P453497	-1.116389	-1.165439	RNA binding motif protein 20
RNF182	A_23_P399255	-2.692754	-2.238002	ring finger protein 182
SLC45A3	A_24_P208345	-1.514775	-1.182414	solute carrier family 45 member 3
SLC4A10	A_24_P930111	-2.103964	-2.200479	solute carrier family 4 member 10
SLC4A10	A_24_P314786	-1.750496	-1.796706	solute carrier family 4 member 10
THSD7A	A_24_P400324	-1.690056	-1.149354	thrombospondin type 1 domain containing 7A
TRIM49	A_23_P1575	-2.460168	-2.278707	tripartite motif containing 49
TRIM51	A_23_P150483	-2.767962	-2.201392	tripartite motif-containing 51
TRIM53AP	A_24_P16353	-2.039508	-2.085168	tripartite motif containing 53A, pseudogene
TRIM64	A_23_P12972	-2.396233	-2.756967	tripartite motif containing 64
TRPM6	A_23_P216712	-2.766311	-2.765324	transient receptor potential cation channel subfamily M member 6
UGT2B11	A_23_P212968	-1.109849	-1.055996	UDP glucuronosyltransferase family 2 member B11
UGT2B7	A_23_P136671	-1.281892	-2.223901	UDP glucuronosyltransferase family 2 member B7
VWCE	A_23_P52986	-1.113653	-1.94727	von Willebrand factor C and EGF domains
ZNF91	A_23_P209146	-1.06124	-1.009823	zinc finger protein 91

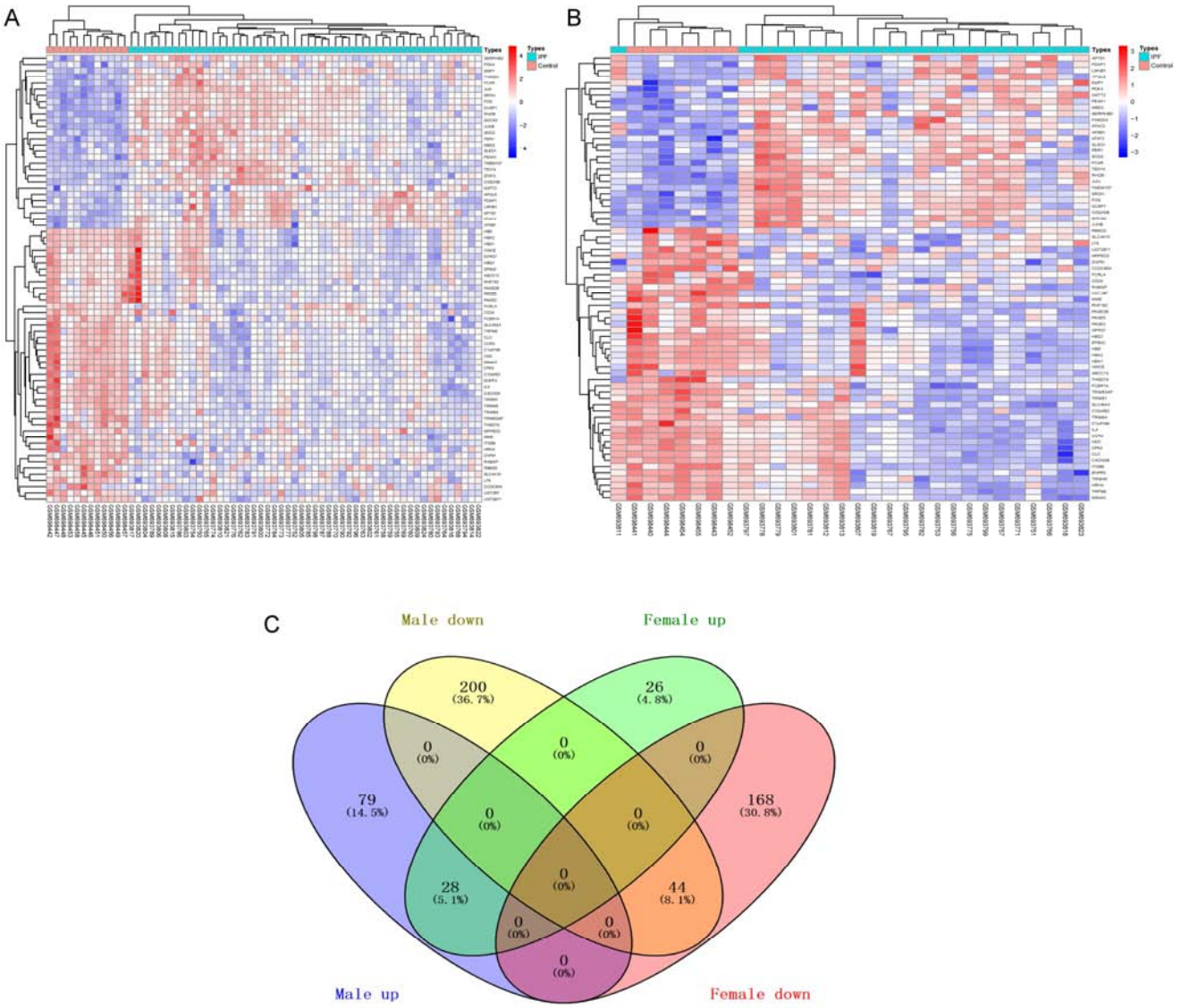

Figure 1. *A heatmap of 72 differentially expressed genes between IPF patients and healthy controls. (A) Male IPF patients and male healthy controls. (B) Female IPF patients and female healthy controls. Red represents upregulated genes, and blue represents downregulated genes. (C) Venn diagram of differentially expressed genes between IPF patients and healthy controls. Up represents upregulated genes, and down represents downregulated genes.*

3.2. Go and Pathway Enrichment Analysis of DEGs

To analyze the functions and mechanisms of DEGs, the functional and pathway enrichment analyses of upregulated and downregulated DEGs were performed using the DAVID 6.8 online tool. In our study, a total of 51 GO terms and 8 pathways of DEGs (P-value <0.05), including 27 BPs, 12 CCs, and 12 MFs, were obtained, and the top five of each item are shown in Table 3. GO analysis results showed that changes in BPs of upregulated DEGs were significantly enriched in response to cAMP, positive regulation of cell differentiation, cellular response to calcium ion, response to drug, and regulation of cell cycle. Downregulated DEGs in BPs were significantly enriched in oxygen transport, bicarbonate transport, positive regulation of mast cell degranulation, angiotensin maturation, and positive regulation of cytosolic calcium ion concentration. Changes in CCs of upregulated DEGs were mainly enriched in nuclear chromatin, lamin filament, ciliary transition zone, transcription factor complex, and nuclear inner membrane. Downregulated DEGs in CCs were mainly enriched in hemoglobin complex, haptoglobin-hemoglobin complex, integral component of plasma membrane, endocytic vesicle lumen, and blood microparticle. Changes in MFs of upregulated DEGs were mainly enriched in RNA polymerase II core promoter proximal region sequence-specific DNA binding, transcription factor activity, RNA polymerase II core promoter proximal region sequence-specific binding, transcriptional activator activity, RNA polymerase II core promoter proximal region sequence-specific binding, and transcription factor binding. Changes in MFs of downregulated DEGs were mainly enriched in oxygen transporter activity, oxygen binding, heme binding, iron ion binding, and haptoglobin binding (Table 3).

The pathways enriched by upregulated DEGs were mainly related to the TNF signaling pathway, Osteoclast differentiation, Herpes simplex infection, Prolactin signaling

pathway, and Hepatitis B. The pathways enriched by downregulated DEGs were mainly related to Asthma, Fc epsilon RI signaling pathway, and Hematopoietic cell lineage (Table 3).

Table 3. *The top five GO and pathway enrichment analysis of DEGs.*

Category	Term	Description	Count	P. Value
Upregulated genes				
GOTERM_BP	GO:0051591	response to cAMP	3	0.0000928
GOTERM_BP	GO:0045597	positive regulation of cell differentiation	3	0.0003071
GOTERM_BP	GO:0071277	cellular response to calcium ion	3	0.0010256
GOTERM_BP	GO:0042493	response to drug	3	0.0055356
GOTERM_BP	GO:0051726	regulation of cell cycle	3	0.0055356
GOTERM_CC	GO:0000790	nuclear chromatin	4	0.0023008
GOTERM_CC	GO:0005638	lamin filament	2	0.0086248
GOTERM_CC	GO:0035869	ciliary transition zone	2	0.0273487
GOTERM_CC	GO:0005667	transcription factor complex	3	0.0309618
GOTERM_CC	GO:0005637	nuclear inner membrane	2	0.0374182
GOTERM_MF	GO:0000978	RNA polymerase II core promoter proximal region sequence-specific DNA binding	6	0.0001178
GOTERM_MF	GO:0000982	transcription factor activity, RNA polymerase II core promoter proximal region sequence-specific binding	2	0.0293031
GOTERM_MF	GO:0001077	transcriptional activator activity, RNA polymerase II core promoter proximal region sequence-specific binding	3	0.0412042
GOTERM_MF	GO:0008134	transcription factor binding	2	0.0483833
KEGG_PATHWAY	ptr04668	TNF signaling pathway	4	0.0003942
KEGG_PATHWAY	ptr04380	Osteoclast differentiation	4	0.0007797
KEGG_PATHWAY	ptr05168	Herpes simplex infection	4	0.0022599
KEGG_PATHWAY	ptr04917	Prolactin signaling pathway	3	0.0042762
KEGG_PATHWAY	ptr05161	Hepatitis B	3	0.0186064
Downregulated genes				
GOTERM_BP	GO:0015671	oxygen transport	4	0.0000031
GOTERM_BP	GO:0015701	bicarbonate transport	3	0.0033648
GOTERM_BP	GO:0043306	positive regulation of mast cell degranulation	2	0.0214126
GOTERM_BP	GO:0002003	angiotensin maturation	2	0.0214126
GOTERM_BP	GO:0007204	positive regulation of cytosolic calcium ion concentration	3	0.0284004
GOTERM_CC	GO:0005833	hemoglobin complex	4	0.0000015
GOTERM_CC	GO:0031838	haptoglobin-hemoglobin complex	2	0.0078789
GOTERM_CC	GO:0005887	integral component of plasma membrane	8	0.0190709
GOTERM_CC	GO:0071682	endocytic vesicle lumen	2	0.0311553
GOTERM_CC	GO:0072562	blood microparticle	3	0.0361847
GOTERM_MF	GO:0005344	oxygen transporter activity	4	0.0000032
GOTERM_MF	GO:0019825	oxygen binding	4	0.0001354
GOTERM_MF	GO:0020037	heme binding	4	0.0030695
GOTERM_MF	GO:0005506	iron ion binding	4	0.0041867
GOTERM_MF	GO:0031720	haptoglobin binding	2	0.0063845
KEGG_PATHWAY	hsa05310	Asthma	3	0.0026938
KEGG_PATHWAY	hsa04664	Fc epsilon RI signaling pathway	3	0.0133022
KEGG_PATHWAY	hsa04640	Hematopoietic cell lineage	3	0.0212146

If there were more than five terms enriched in this category, the top five terms were selected according to P-value.

3.3. PPI Network Construction and Hub Gene Identification

Protein interactions among the DEGs were predicted with STRING online database. A PPI network with 69 nodes and 68 edges was obtained and the PPI network was visualized by Cytoscape (Figure 2B). The cytoHubba plugin was then used to analyze hub genes with MCC, and genes with the top 10 scores were identified as hub genes (Figure 2C). As shown in Figure 2C, six upregulated genes (JUN, FOS, STAT3, SOCS3, JUNB, DUSP1) and four downregulated genes (IL4, FCER1A, MS4A2, CPA3) were identified. The gene symbols, full names, and scores of hub genes are shown in Table 4.

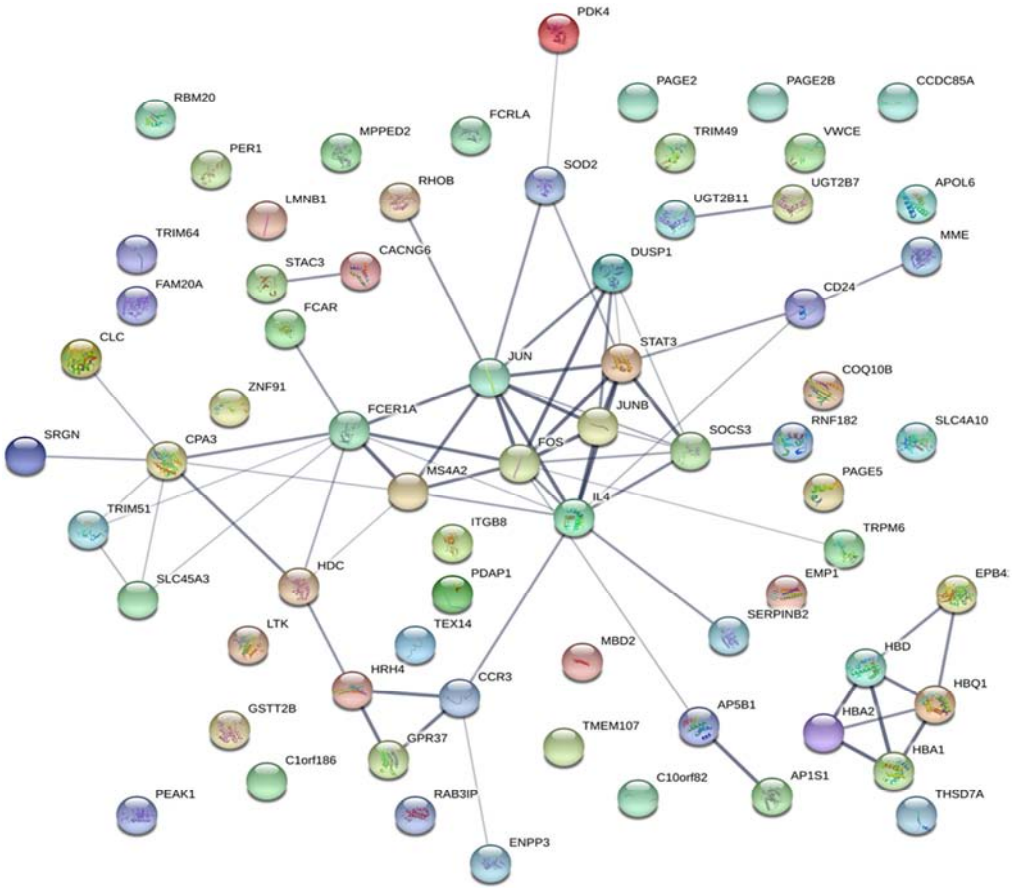
PDK4
PAGE2
PAGE2B
CCDC85A
RBM20
FCRLA
MPPED2
TRIM49
VWCE
PER1
SOD2
RHOB
UGT2B7
APOL6
LMNB1
UGT2B11
TRIM64
MME
CACNG6
DUSP1
STAC3
FAM20A
CD24
FCAR
CLC
STAT3
JUN
COQ10B
ZNF91
JUNB
FCER1A
RNF182
SLC4A10
SRGN
CPA3
FOS
SOCS3
MS4A2
PAGE5
IL4
TRIM51
ITGB8
TRPM6
HDC
EMP1
EPB4
SLC45A3
PDAP1
SERPINB2
LTK
TEX14
MBD2
HBD
HRH4
CCR3
HBQ1
AP5B1
GSTT2B
HBA2
TMEM107
GPR37
HBA1
C1orf186
C10orf82
AP1S1
PEAK1
RAB3IP
THSD7A
ENPP3

A

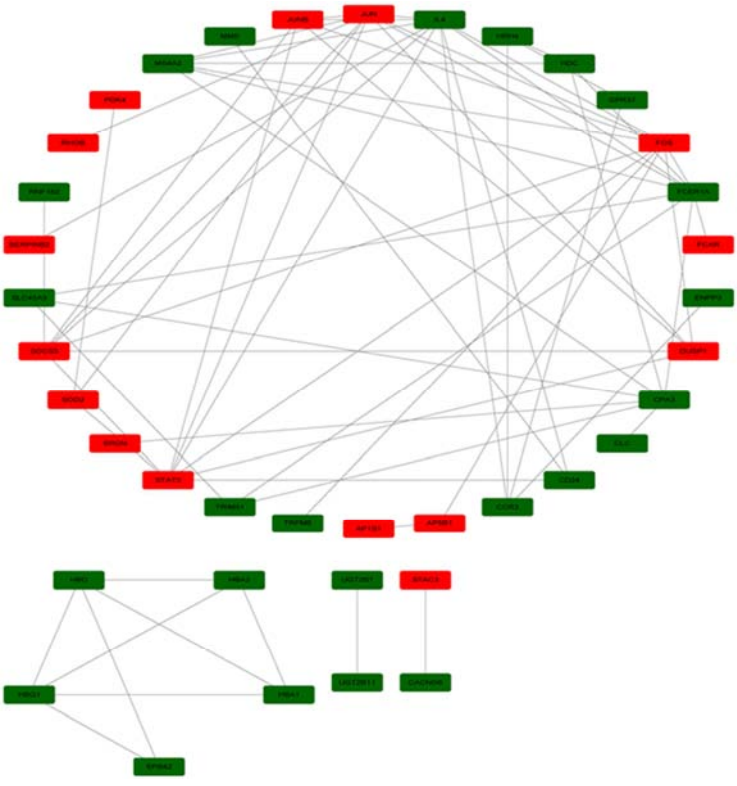

B

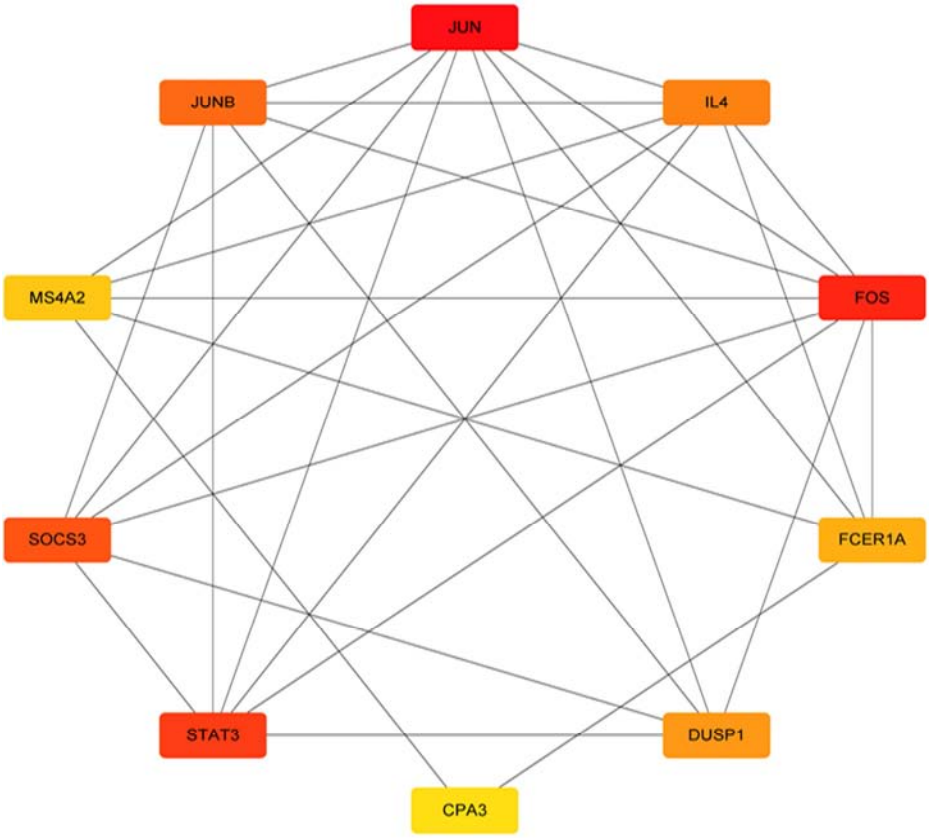

C

Figure 2. *PPI network construction and bub gene identification. (A) PPI network for DEGs. (B) Cytoscape network visualization of the 69 nodes and 68 edges that were obtained with interaction scores >0.4 according to the STRING online database. The nodes represent genes, and the edges represent links between genes. Red represents upregulated genes, and green represents downregulated genes. (C) The hub genes with the top 10 scores.*

Table 4. *The top 10 hub genes with highest scores.*

Gene symbol	Full name	Score
JUN	Jun proto-oncogene, AP-1 transcription factor subunit	267
FOS	Fos proto-oncogene, AP-1 transcription factor subunit	266
STAT3	signal transducer and activator of transcription 3	244
SOCS3	suppressor of cytokine signaling 3	241
JUNB	JunB proto-oncogene, AP-1 transcription factor subunit	240
IL4	interleukin 4	148
DUSP1	dual specificity phosphatase 1	120
FCER1A	Fc fragment of IgE receptor Ia	37
MS4A2	membrane spanning 4-domains A2	30
CPA3	carboxypeptidase A3	14

3.4. Go and Pathway Enrichment Analysis of Hub Genes

We performed a functional enrichment analysis for hub genes. The GO analysis demonstrated that changes in BPs were mainly enriched in cellular response to calcium ion, regulation of cell cycle, positive regulation of mast cell degranulation, response to muscle stretch, B cell activation, positive regulation of pri-miRNA transcription from RNA polymerase II promoter, positive regulation of cell differentiation, SMAD protein signal transduction, transforming growth factor beta receptor signaling pathway, and response to drug. Changes in CCs were significantly enriched in external side of plasma membrane and nucleoplasm. Changes in MFs for the hub genes were enriched mainly in transcriptional activator activity, RNA polymerase II core promoter proximal region sequence-specific binding, and RNA polymerase II core promoter proximal region sequence-specific DNA binding.

The pathways enriched by hub genes were mainly related to Asthma, Fc epsilon RI signaling pathway, Inflammatory bowel disease (IBD), Leishmaniasis, T cell receptor signaling pathway, TNF signaling pathway, Osteoclast differentiation, Jak-STAT signaling pathway, Prolactin signaling pathway, Measles, Hepatitis B, Herpes simplex infection, and MAPK signaling pathway (Table 5).

Table 5. *GO and pathway enrichment analysis of hub genes.*

Category	Term	Description	Count	P. Value
GOTERM_BP	GO:0071277	cellular response to calcium ion	3	0.00022
GOTERM_BP	GO:0051726	regulation of cell cycle	3	0.0009196
GOTERM_BP	GO:004330	positive regulation of mast cell degranulation	2	0.0067371
GOTERM_BP	GO:0035994	response to muscle stretch	2	0.0075764
GOTERM_BP	GO:0042113	B cell activation	2	0.0092531
GOTERM_BP	GO:1902895	positive regulation of pri-miRNA transcription from RNA polymerase II promoter	2	0.0100905
GOTERM_BP	GO:0045597	positive regulation of cell differentiation	2	0.0109273
GOTERM_BP	GO:0060395	SMAD protein signal transduction	2	0.0267071
GOTERM_BP	GO:0007179	transforming growth factor beta receptor signaling pathway	2	0.0390064
GOTERM_BP	GO:0042493	response to drug	2	0.0430753
GOTERM_CC	GO:0009897	external side of plasma membrane	3	0.0043499
GOTERM_CC	GO:0005654	nucleoplasm	4	0.0406351
GOTERM_MF	GO:0001077	transcriptional activator activity, RNA polymerase II core promoter proximal region sequence-specific binding	3	0.0033735
GOTERM_MF	GO:0000978	RNA polymerase II core promoter proximal region sequence-specific DNA binding	3	0.0066624
KEGG_PATHWAY	hsa05310	Asthma	4	0.0000139
KEGG_PATHWAY	hsa04664	Fc epsilon RI signaling pathway	4	0.0000653
KEGG_PATHWAY	hsa05321	Inflammatory bowel disease (IBD)	4	0.0001043
KEGG_PATHWAY	hsa05140	Leishmaniasis	4	0.0001407
KEGG_PATHWAY	hsa04660	T cell receptor signaling pathway	4	0.0002361
KEGG_PATHWAY	hsa04668	TNF signaling pathway	4	0.000313
KEGG_PATHWAY	hsa04380	Osteoclast differentiation	4	0.0004247
KEGG_PATHWAY	hsa04630	Jak-STAT signaling pathway	4	0.0010633
KEGG_PATHWAY	hsa04917	Prolactin signaling pathway	3	0.0048486
KEGG_PATHWAY	hsa05162	Measles	3	0.0124324
KEGG_PATHWAY	hsa05161	Hepatitis B	3	0.014251
KEGG_PATHWAY	hsa05168	Herpes simplex infection	3	0.0322808
KEGG_PATHWAY	hsa04010	MAPK signaling pathway	3	0.0400919

3.5. Using Hub Genes for IPF Diagnosis

The diagnostic accuracy of the top 10 hub genes was assessed using ROC curve analysis (Figure 3). The areas under the ROC curves were 0.9797, 0.9629, 0.9654, 0.9687, and 0.9154 for JUN, FOS, JUNB, SOCS3, and STAT3, as shown in Figure 3A. The areas under the ROC curves were 0.9318, 0.9501, 0.8805, 0.932, and 0.9365 for DUSP1, IL4, FCER1A, MS4A2, and CPA3, as shown in Figure 3B.

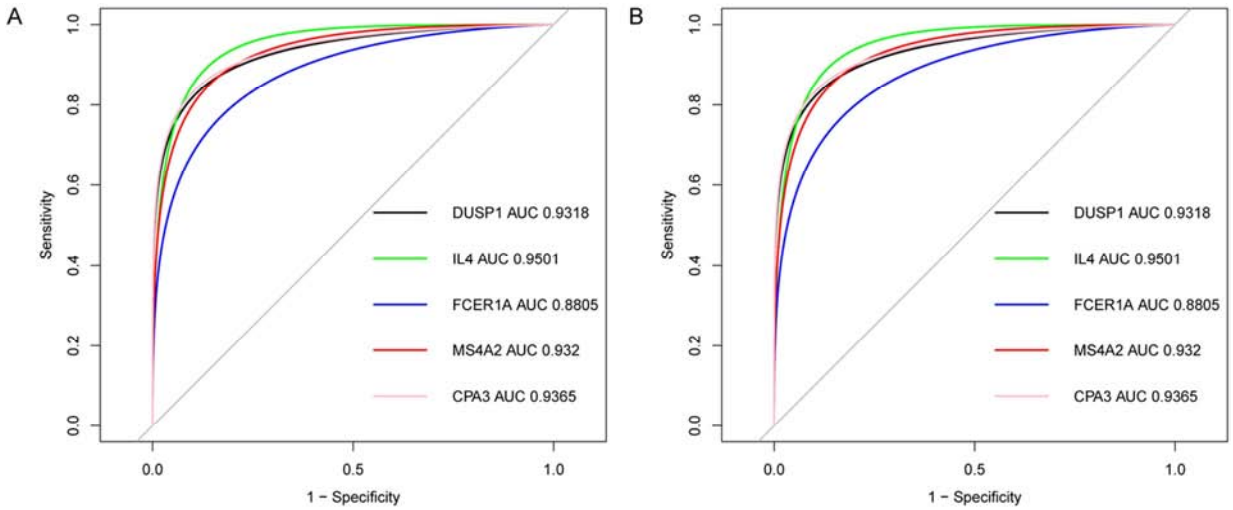

Figure 3. *Validation of the diagnostic value of the hub genes for IPF. (A-B) Receiver operating characteristic curve of the hub genes for diagnosis of IPF.*

4. Discussion

In this study, we analyzed the DEGs in PBMCs from IPF patients and healthy controls. We performed independently for the male IPF and female IPF patients to pinpoint the potential gens. The results of the microarray analysis revealed the expression of 72 DEGs (28 upregulated genes and 44 downregulated genes). The associations between these genes were revealed by constructing a PPI network. The top 10 genes with the highest scores were identified, including JUN, FOS, STAT3, SOCS3, JUNB, DUSP1, IL4, FCER1A, MS4A2, and CPA3. There were six upregulated genes (JUN, FOS, STAT3, SOCS3, JUNB, DUSP1) and four downregulated genes (IL4,

FCER1A, MS4A2, CPA3). In addition, we use GO and pathway enrichment analysis to perform their functions. At the same time, we used the ROC curve to analyze the AUC of the 10 top hub genes.

JUN, FOS, STAT3, SOCS3, JUNB, and DUSP1 are upregulated genes in PBMC of IPF. JUN and FOS are a subunit of the activator protein-1 (AP-1) [14]. AP-1 is a dimeric complex composed of the JUN (c-JUN, JUND, JUNB), FOS, ATF, and MAF protein families [14-16]. It can be seen that JUNB is a member of the JUN protein. Moreover, JUN and FOS are important members of the transcription AP-1 [17]. One study has reported that AP-1 induction may be associated with increased proliferation and extracellular matrix (ECM) production in IPF fibroblasts [18]. And Werning et al. have recently found that c-JUN and FOS are expressed in fibroblasts of IPF [19]. Besides, Chang et al. have shown that JUNB can regulate Epithelial-to-mesenchymal transition (EMT) [20]. One study has shown that EMT plays an important role in the pathogenesis of IPF [21]. Therefore, JUN, FOS, and JUNB may be involved in forming IPF.

STAT3 is a ubiquitously expressed latent cytoplasmic protein that regulates lung fibrosis [22]. Waters et al. have shown that STAT3 can promote fibroblast senescence to promote fibrosis [23]. Milara et al. have found that lung from patients with IPF expressed higher levels of STAT3, as well as phosphorylated [24]. Recently, it has been demonstrated that STAT3 regulates lung fibroblast-myofibroblast activation and differentiation in IPF [25]. Given these findings, STAT3 can be used as a biomarker in IPF.

SOCS3 is one of the most studied members of the SOCS family that consists of eight proteins (SOCS1-7 and cytokine-inducible SH2-containing protein, CISH) [26]. SOCS3 can be a major regulator of STAT3 activation [27]. One study has found that SOCS3 expression was shown to be elevated for up to 30 days in bleomycin-induced fibrosis [28]. A study by Akram et al. has shown that a significant increase in SOCS3 expression was observed in IPF AEC and macrophages compared to control lung tissue using dual immunohistochemical analysis [29]. Shocher et al. have found that primary human fibroblast culture from IPF (IPF-HLFs) expressed higher levels of SOCS3 when tested basal levels in HLFs [30]. Therefore, it may be hypothesized that SOCS3 may play a significant role in IPF.

DUSP1, also named mitogen-activated protein kinase (MAPK) phosphatase (MKP-1) that dephosphorylates and deactivate MAPKs, acts as a negative regulator of the MAPK signaling pathway [31, 32]. Redente et al. have shown that DUSP1-deficient mice reduced pulmonary fibrosis in bleomycin-induced fibrosis and pulmonary fibrosis was attenuated in mice given bleomycin using DUSP1 inhibitors [33]. Besides, one study has found that DUSP1 plays a critical role in promoting pulmonary fibrosis from macrophages to fibroblasts in vivo experiments [34]. These studies suggest that DUSP1 plays a crucial role in IPF and maybe a relevant therapeutic target.

IL4, FCER1A, MS4A2, and CPA3 are downregulated genes in PBMC of IPF. IL-4 is a fibrogenic cytokine that increases collagen production by fibroblasts [35]. But one study has found that pulmonary fibrosis and lung injury and inflammation in the bleomycin-induced fibrosis model of IL-4-deficient mice were substantially less than wild-type mice [36]. These results suggest that IL-4 has both fibrogenic and anti-inflammatory in the context of bleomycin-induced lung fibrosis and injury. FCER1A gene encodes the a-subunit (FCER1a) of the high-affinity IgE receptor consisting of an a-chain (FCER1), an β-chain (MS4A2) and two γ-chains (FCER1G) [37-39]. FCER1 and AMS4A2 expressing in mast cells (MCs) are associated with asthma [37, 38, 40]. But CPA3 is one of the MC-restricted proteases that are secreted by MCs [41]. It is also associated with asthma [41]. What's more, it is demonstrated that FCER1A, MS4A2, and CPA3 may be favorable prognostic indicators in non-small cell lung cancer [42, 43]. However, there is no research on the relationship between FCER1A, MS4A2, and CPA3 and IPF so far. Based on our study, we can predict that FCER1A, MS4A2, and CPA3 may be PBMC markers in IPF.

In our study, all the AUC values of the top 10 genes were in the range 0.880-0.980 concerning the ROC curve. These genes possess high accuracy except that FCER1A indicated moderate accuracy [44]. KEGG enrichment analysis of these genes showed that these genes were mainly linked to the Fc epsilon RI signaling pathway, TNF signaling pathway, Jak-STAT signaling pathway, and MAPK signaling pathway. These signaling pathways play an essential role in the pathogenesis of IPF. We speculated that these genes might play an important role in IPF. But our study has a few limitations. Firstly, to fully identify the key genes in PBMC of IPF, it is better to combine venous blood samples and lung tissue to explore. Second, the sample size of the dataset we explored was too small. Therefore, it is necessary to increase the samples to improve the diagnostic accuracy of these hub genes in IPF. Third, a single microarray analysis was used in our study. It may result in a high false-positive rate. Thus, it is necessary to improve the detection capability by combining multiple individual data in future studies. What's more, some key genes and pathways were not found in IPF in previous studies. For this reason, we need more experimental evidence to prove the relationship between these key genes and IPF.

5. Conclusion

Our study used bioinformatics analysis to identify the associated biological functions and pathways involved in IPF to explore the pathogenesis, diagnosis, and prognosis of IPF. Moreover, we identified 10 key genes as potential diagnostic biomarkers through PPI network analysis and the ROC curve analysis. However, more experiments are needed to validate the results of our study further.

Acknowledgements

The authors would like to express their sincere thanks to all those who have lent them hands in writing this paper.

References

[1] Raghu G, Collard HR, Egan JJ, et al. An official ATS/ERS/JRS/ALAT statement: idiopathic pulmonary fibrosis: evidence-based guidelines for diagnosis and management. Am J Respir Crit Care Med, 2011, 183 (6): 788-824.

[2] Lederer DJ, Martinez FJ. Idiopathic Pulmonary Fibrosis. N Engl J Med, 2018, 378 (19): 1811-1823.

[3] Richeldi L, Collard HR, Jones MG. Idiopathic pulmonary fibrosis. Lancet, 2017, 389 (10082): 1941-1952.

[4] Hutchinson J, Fogarty A, Hubbard R, et al. Global incidence and mortality of idiopathic pulmonary fibrosis: a systematic review. Eur Respir J, 2015, 46 (3): 795-806.

[5] American Thoracic Society/European Respiratory Society International Multidisciplinary Consensus Classification of the Idiopathic Interstitial Pneumonias. This joint statement of the American Thoracic Society (ATS), and the European Respiratory Society (ERS) was adopted by the ATS board of directors, June 2001 and by the ERS Executive Committee, June 2001. Am J Respir Crit Care Med, 2002, 165 (2): 277-304.

[6] Sgalla G, Iovene B, Calvello M, et al. Idiopathic pulmonary fibrosis: pathogenesis and management. Respir Res, 2018, 19 (1): 32.

[7] Wolters PJ, Collard HR, Jones KD. Pathogenesis of idiopathic pulmonary fibrosis. Annu Rev Pathol, 2014, 9: 157-79.

[8] Wolters PJ, Blackwell TS, Eickelberg O, et al. Time for a change: is idiopathic pulmonary fibrosis still idiopathic and only fibrotic? Lancet Respir Med, 2018, 6 (2): 154-160.

[9] Qiu CC, Su QS, Zhu SY, et al. Identification of Potential Biomarkers and Biological Pathways in Juvenile Dermatomyositis Based on miRNA-mRNA Network. Biomed Res Int, 2019, 2019: 7814287.

[10] Zhang G, Xu S, Zhang Z, et al. Identification of Key Genes and the Pathophysiology Associated With Major Depressive Disorder Patients Based on Integrated Bioinformatics Analysis. Front Psychiatry, 2020, 11: 192.

[11] Yi XH, Zhang B, Fu YR, et al. STAT1 and its related molecules as potential biomarkers in Mycobacterium tuberculosis infection. J Cell Mol Med, 2020, 24 (5): 2866-2878.

[12] Ashburner M, Ball CA, Blake JA, et al. Gene ontology: tool for the unification of biology. The Gene Ontology Consortium. Nature genetics, 2000, 25 (1): 25-29.

[13] Kanehisa M, Goto S. KEGG: kyoto encyclopedia of genes and genomes. Nucleic acids research, 2000, 28 (1): 27-30.

[14] Eferl R, Wagner EF. AP-1: a double-edged sword in tumorigenesis. Nat Rev Cancer, 2003, 3 (11): 859-68.

[15] Shaulian E. AP-1 — The Jun proteins: Oncogenes or tumor suppressors in disguise? Cellular Signalling, 2010, 22 (6): 894-899.

[16] Gazon H, Barbeau B, Mesnard JM, et al. Hijacking of the AP-1 Signaling Pathway during Development of ATL. Front Microbiol, 2017, 8: 2686.

[17] Jiang X, Xie H, Dou Y, et al. Expression and function of FRA1 protein in tumors. Mol Biol Rep, 2020, 47 (1): 737-752.

[18] Klymenko O, Huehn M, Wilhelm J, et al. Regulation and role of the ER stress transcription factor CHOP in alveolar epithelial type-II cells. J Mol Med (Berl), 2019, 97 (7): 973-990.

[19] Wernig G, Chen SY, Cui L, et al. Unifying mechanism for different fibrotic diseases. Proc Natl Acad Sci U S A, 2017, 114 (18): 4757-4762.

[20] Chang H, Liu Y, Xue M, et al. Synergistic action of master transcription factors controls epithelial-to-mesenchymal transition. Nucleic Acids Res, 2016, 44 (6): 2514-27.

[21] Salton F, Volpe MC, Confalonieri M. Epithelial-Mesenchymal Transition in the Pathogenesis of Idiopathic Pulmonary Fibrosis. Medicina (Kaunas), 2019, 55 (4).

[22] Knight D, Mutsaers SE, Prêle CM. STAT3 in tissue fibrosis: is there a role in the lung? Pulm Pharmacol Ther, 2011, 24 (2): 193-8.

[23] Waters DW, Blokland KEC, Pathinayake PS, et al. Fibroblast senescence in the pathology of idiopathic pulmonary fibrosis. Am J Physiol Lung Cell Mol Physiol, 2018, 315 (2): L162-l172.

[24] Milara J, Hernandez G, Ballester B, et al. The JAK2 pathway is activated in idiopathic pulmonary fibrosis. Respir Res, 2018, 19 (1): 24.

[25] Pechkovsky DV, Prêle CM, Wong J, et al. STAT3-mediated signaling dysregulates lung fibroblast-myofibroblast activation and differentiation in UIP/IPF. Am J Pathol, 2012, 180 (4): 1398-412.

[26] Yoshimura A, Naka T, Kubo M. SOCS proteins, cytokine signalling and immune regulation. Nat Rev Immunol, 2007, 7 (6): 454-65.

[27] Rottenberg ME, Carow B. SOCS3 and STAT3, major controllers of the outcome of infection with Mycobacterium tuberculosis. Semin Immunol, 2014, 26 (6): 518-32.

[28] O'Donoghue RJ, Knight DA, Richards CD, et al. Genetic partitioning of interleukin-6 signalling in mice dissociates Stat3 from Smad3-mediated lung fibrosis. EMBO Mol Med, 2012, 4 (9): 939-51.

[29] Akram KM, Lomas NJ, Forsyth NR, et al. Alveolar epithelial cells in idiopathic pulmonary fibrosis display upregulation of TRAIL, DR4 and DR5 expression with simultaneous preferential over-expression of pro-apoptotic marker p53. Int J Clin Exp Pathol, 2014, 7 (2): 552-64.

[30] Shochet GE, Brook E, Bardenstein-Wald B, et al. TGF-β pathway activation by idiopathic pulmonary fibrosis (IPF) fibroblast derived soluble factors is mediated by IL-6 trans-signaling. Respir Res, 2020, 21 (1): 56.

[31] Moosavi SM, Prabhala P, Ammit AJ. Role and regulation of MKP-1 in airway inflammation. Respir Res, 2017, 18 (1): 154.

[32] Keyse SM. Dual-specificity MAP kinase phosphatases (MKPs) and cancer. Cancer Metastasis Rev, 2008, 27 (2): 253-61.

[33] Redente EF, Black BP, Aguilar MA, et al. DUSP1 inhibition impairs fibrosis development by altering macrophage programming. American Journal of Respiratory and Critical Care Medicine, 2017, 195.

[34] Goda C, Balli D, Black M, et al. Loss of FOXM1 in macrophages promotes pulmonary fibrosis by activating p38 MAPK signaling pathway. PLoS Genetics, 2020, 16 (4).

[35] Tsoutsou PG, Gourgoulianis KI, Petinaki E, et al. Cytokine levels in the sera of patients with idiopathic pulmonary fibrosis. Respir Med, 2006, 100 (5): 938-45.

[36] Huaux F, Liu T, McGarry B, et al. Dual roles of IL-4 in lung injury and fibrosis. J Immunol, 2003, 170 (4): 2083-92.

[37] Kraft S, Kinet JP. New developments in FcepsilonRI regulation, function and inhibition. Nat Rev Immunol, 2007, 7 (5): 365-78.

[38] Potaczek DP, Michel S, Sharma V, et al. Different FCER1A polymorphisms influence IgE levels in asthmatics and non-asthmatics. Pediatr Allergy Immunol, 2013, 24 (5): 441-9.

[39] Wu LC, Zarrin AA. The production and regulation of IgE by the immune system. Nat Rev Immunol, 2014, 14 (4): 247-59.

[40] Ferreira MA, Zhao ZZ, Thomsen SF, et al. Association and interaction analyses of eight genes under asthma linkage peaks. Allergy, 2009, 64 (11): 1623-8.

[41] Pejler G. The emerging role of mast cell proteases in asthma. Eur Respir J, 2019, 54 (4).

[42] Ly D, Zhu CQ, Cabanero M, et al. Role for High-Affinity IgE Receptor in Prognosis of Lung Adenocarcinoma Patients. Cancer Immunol Res, 2017, 5 (9): 821-829.

[43] Visser S, Hou J, Bezemer K, et al. Prediction of response to pemetrexed in non-small-cell lung cancer with immunohistochemical phenotyping based on gene expression profiles. BMC Cancer, 2019, 19 (1): 440.

[44] Akobeng AK. Understanding diagnostic tests 3: Receiver operating characteristic curves. Acta Paediatr, 2007, 96 (5): 644-7.